PCSK9 deficiency results in a specific shedding of excess LDLR in female mice only: Role of hepatic cholesterol

Anna Roubtsova, Damien Garçon, Sandrine Lacoste, Ann Chamberland, Jadwiga Marcinkiewicz, Raphaël Métivier, Thibaud Sotin, Martine Paquette, Sophie Bernard, Bertrand Cariou, et al.

PCSK9 deficiency results in a specific shedding of excess LDLR in female mice only: role of hepatic cholesterol

Anna Roubtsova[1], Damien Garçon[1], Sandrine Lacoste[1,5], Ann Chamberland[1], Jadwiga Marcinkiewicz[1], Raphaël Métivier[2], Thibaud Sotin[1,3], Martine Paquette[1], Sophie Bernard[1], Bertrand Cariou[3], Cédric Le May[3], Marlys L. Koschinsky[4], Nabil G. Seidah[1] and Annik Prat[1]*

[1]*Institut de Recherches Cliniques de Montréal (IRCM), affiliated to the Université de Montréal, Montreal, QC, Canada*
[2]*Equipe SP@RTE, UMR 6290 CNRS, Université de Rennes 1, Rennes, France*
[3]*Nantes Université, CHU Nantes, CNRS, INSERM, l'Institut du thorax, F-44000 Nantes, France*
[4]*Robarts Research Institute, Schulich School of Medicine & Dentistry, Western University, London, ON, Canada*
[5]*S.L. present address: Centre de recherche de l'hôpital Maisonneuve Rosemont, Montreal, QC, Canada*

Short title: **Sex-dependent regulation of hepatic membrane LDLR**

*Correspondence to Annik Prat, IRCM, 110 Pine Avenue West, Montreal (QC), Canada H2W 1R7; Annik.Prat@ircm.qc.ca

ABSTRACT

PCSK9 promotes the lysosomal degradation of cell surface LDL receptor (LDLR). We analyzed how excess LDLR generated by PCSK9 deficiency is differently handled in male and female mice to possibly unveil the mechanism leading to the lower efficacy of PCSK9 mAb on LDL-cholesterol levels in women. Analysis of intact or ovariectomized PCSK9 knockout (KO) mice supplemented with placebo or 17β-estradiol (E2) demonstrated that female, but not male mice massively shed the soluble ectodomain of the LDLR in the plasma. Liver-specific PCSK9 KO or alirocumab-treated WT mice exhibit the same pattern. This shedding is distinct from the basal one and is inhibited by ZLDI-8, a metalloprotease inhibitor pointing at ADAM10/ADAM17. In PCSK9 KO female mice, ZLDI-8 raises by 80% the LDLR liver content in a few hours. This specific shedding is likely cholesterol-dependent: it is prevented in PCSK9 KO male mice that exhibit low intra-hepatic cholesterol levels without activating SREBP-2, and enhanced by mevalonate or high cholesterol feeding, or by E2 known to stimulate cholesterol synthesis via the estrogen receptor-α. Liver transcriptomics demonstrates that critically low liver cholesterol in ovariectomized female or knockout male mice also hampers the cholesterol-dependent G2/M transition of the cell cycle. Finally, higher levels of shed LDLR were measured in the plasma of women treated with PCSK9 mAb. PCSK9 knockout female mice hormonally sustain cholesterol synthesis and shed excess LDLR, seemingly like women. In contrast, male mice rely on high surface LDLR to replenish their stocks, despite 80% lower circulating LDL.

Keywords: soluble LDLR, estrogen, ERalpha, cholesterogenesis, hepatocyte proliferation.

Abbreviations: mAb, monoclonal antibody; DEG, differentially expressed gene; E2, 17β-estradiol; ER, endoplasmic reticulum; ERα, estrogen receptor alpha; Gper1, G protein-coupled estrogen receptor 1; KO, knockout; LDL-C, LDL-cholesterol; LDLR, low density lipoprotein receptor; Ovx, ovariectomy; OvxP, ovariectomized and supplemented with placebo; PCSK9, proprotein convertase of the subtilisin/kexin type 9; sLDLR, shed LDLR. WT, wild-type.

1. Introduction

The uptake of cholesterol-rich LDLs by the liver is a key process that protects from atherosclerosis. The liver expresses ~70% of the whole-body LDL receptor (LDLR), and the cell surface density of the receptor in this tissue is a major determinant for LDL clearance by endocytosis. Aside from its exquisite transcriptional regulation [1], cell surface LDLR is tightly regulated in this organ by different mechanisms of post-translational degradation. The strongest regulation is exerted by PCSK9. This protein belongs to the proprotein convertase family of serine proteases [2], but has only itself as a substrate [3]. PCSK9 is mainly expressed in hepatocytes, but is also abundant in the intestinal epithelium, pancreatic islets, and kidneys [4]. However, these other tissues do not significantly contribute to circulating PCSK9 [5], which only originates from the liver [6]. PCSK9 binds the cell surface LDLR in the liver or peripheral tissues [7], this complex is then internalized in endosomes, and eventually degraded in lysosomes [8,9]. Gain-of-function mutations of PCSK9 lead to familial hypercholesterolemia [10], due to reduced LDL-cholesterol (LDL-C) clearance from circulation. Conversely, loss [11] or inhibition [12] of PCSK9 results in substantial reductions in LDL-C levels. PCSK9 monoclonal antibodies (mAb) that reduce LDL-C by 50-60% have been prescribed to hypercholesterolemic patients for the last 7 years [13]. Several studies reveal that even though women benefit from PCSK9 lowering therapy as well as men, they often exhibit a 15-20% lower LDL-C reduction when treated with PCSK9 mAbs [14-17]. We also observed sex-specific phenotypes in mice lacking PCSK9. Both male and female livers exhibit 3 to 4-fold higher levels of total LDLR protein [6,18]. However, their cell surface LDLR density greatly differs. It is 4-fold lower in female than in male liver plasma membrane preparations. This sexual dimorphism, which is only observed in the absence of PCSK9, was found to be estrogen-dependent [19].

The present study takes a deep dive into the mechanism behind the 17β-estradiol (E2)-dependent LDLR cell surface density in mice lacking PCSK9. We show that a specific shedding of excess LDLR takes place in female livers only and is likely achieved by the metalloprotease ADAM17. This shedding is distinct from the basal one observed in wild-type (WT) mice or KO male mice. The dissection of the mechanism by which E2 stimulates excess LDLR shedding in PCSK9 KO male mice led us to discover that these mice exhibit critically low cholesterol levels, and that excess LDLR shedding is dependent on cholesterol. Indeed, our data suggest that by

promoting estrogen receptor alpha (ERα)-mediated cholesterogenesis, E2 significantly increases intra-hepatic cholesterol, which in turn stimulates the production of a soluble shed form of the LDLR (sLDLR). Finally, transcriptome analysis of our mouse models revealed that low liver cholesterol in mice lacking PCSK9 was also responsible for delaying the G2/M transition of the cell cycle, known to depend on a cholesterol checkpoint. Finally, sLDLR measurement in the plasma of PCSK9 mAb-treated patients support our hypothesis that lower LDL-C drops in women are due to higher LDLR shedding.

2. Materials and methods

More detailed information on Mice, LDLR immunohistochemistry and RNA-Seq analysis is available in the Supplemental Methods.

2.1. Mice, diets and blood collection

Mice were housed in a 12h-light/dark cycle and fed ad libitum a cholesterol-free standard laboratory diet (2018 Teklad Global; Harlan Laboratories). The IRCM animal care committee approved all procedures. *Pcsk9*$^{+/+}$ (WT) and *Pcsk9*$^{-/-}$ mice were on the C57BL/6J background (≥12 backcrosses) and were F2 littermates of heterozygous breedings [6,18].

2.2. Ovariectomy

Mice underwent sham surgery (sham) or ovariectomy (Ovx) at 8 weeks of age under 2% isoflurane anesthesia (CDMV, Quebec, QC) as described previously [19], except that stainless steel autoclips were used (Becton Dickinson). Two days post-Ovx, mice were re-anesthetized and a pellet delivering either placebo (P) or ~1 μg/day of E2 (E-121, Innovative Research of America, Sarasota, FL) was inserted subcutaneously between the ear and shoulder. The skin was closed with a running 4-0 nylon PDS suture (Ethicon, Bridgewater, NJ) and mice were analyzed 10 to 20 days later.

2.3. LDLR immunohistochemistry

For LDLR visualization, 8 μm-thick frozen liver sections were fixed in 4% paraformaldehyde, rinsed in 0.1% glycine in PBS, washed in PBS, blocked with 1% bovine serum albumin (BSA; Sigma-Aldrich, St. Louis, MO) for 1 h and incubated overnight at 4°C with a goat antibody against mouse LDLR (R&D Systems, Minneapolis, MA). LDLR labeling was visualized by incubation for 1 hour at room temperature with Alexa Fluor 488-labeled donkey anti-goat IgG (Invitrogen, Carlsbad, CA) and nuclei were counterstained with Hoechst Stain solution (Sigma-Aldrich).

2.4. E2, agonist and antagonist treatments

Female mice were distributed in groups of similar average body weights. Cyclodextrin-encapsulated E2 (Sigma-Aldrich) was dissolved in 0.9% NaCl. Propyl pyrazole trisphenol (PPT; Tocris Bioscience, Bristol, UK), G-1 and G15 (Cayman Chemicals, Ann Harbor, MI) were dissolved in DMSO (Sigma-Aldrich) and further diluted to 0.2% DMSO (G1, G15) or 1.28% DMSO (PPT) in saline, ICI 182,780 (Fulvestrant; Sigma-Aldrich) was dissolved in 100% EtOH and diluted to 10% in corn oil.

2.5. Shed LDLR measurement in plasma and in vivo inhibition of metalloproteases

Plasma sLDLR concentration was determined with the DuoSet ELISA (R&D Systems). Male mice were treated with E2 (see above) and male or female mice were treated with the metalloprotease inhibitors BB-94 and ZLDI-8 resuspended in DMSO (MedChemExpress, Princeton, NJ) and diluted ≥10-fold in corn oil before intraperitoneal injection. Control mice received vehicle DMSO in corn oil.

2.6. Plasma and liver cholesterol content

Plasma cholesterol was measured using the Infinity Cholesterol reagent (Fisher Diagnostics, Middletown, VA). For liver cholesterol measurement, tissue (~60 mg) was homogenized in 0.5 mL of chloroform:isopropanol:NP-40 (7:11:0.1) in a micro-homogenizer. The extract was centrifuged at room temperature for 5 min at 19,000 *g*, the supernatant was transferred to a new tube, air dried at 55°C, and vacuum dried in a SpeedVac concentrator. Pellets were resuspended in 0.2 mL of assay buffer of the cholesterol/cholesteryl ester Assay kit (Abcam, Cambridge, UK) using sonication, and 8 µL were assessed as recommended.

2.7. Mevalonate treatment

Mevalonic acid lithium salt (MedChemExpress) was prepared in saline (7.5 mg/mL) and sonicated. Male mice were bled, then gavaged with 0.15 mL saline or mevalonate (35 mg/kg/day) for 9 consecutive days.

2.8. RNA-Seq

Liver pieces (~30 mg; 3 per genotype/condition) were homogenized (Polytron) in 1 mL of TriZol on ice. After addition of 0.2 mL of chloroform, and centrifugation, the upper phase was collected. Contaminating DNA was digested with DNAse I and RNA was purified on Zymo-Spin IIICG columns (ZymoResearch, Irvin, CA). Liver transcripts were chemically fragmented, and cDNA libraries were generated at the Molecular Biology and Functional Genomics platform at the IRCM and randomly sequenced using the Illumina Kit according to the manufacturer's instructions on an Illumina HiSeq 2500 sequencer (PE50).

2.9. Statistical analysis

We first checked the normality and equality of variance of our data with the Shapiro-Wilk test and F-test, respectively. We tested the difference between two groups using parametric unpaired Student's t-test with Welch's correction for unequal variance or non-parametric Mann-Whitney *U* test if required. We assessed comparisons in multi-groups using non-parametric Kruskal-Wallis test followed by Dunn's correction when the normality/equal variance test did not pass, or

using parametric 1-way or 2-way ANOVA followed by Tukey's multiple comparisons test when normality/equal variance tests passed. GraphPad Prism 8 software was used for all analyses. The number of mice used appears in figure legends.

3. Results

3.1. E2 reduces LDLR density at the hepatocyte cell surface primarily via ERα in PCSK9-deficient mice

Higher levels of total liver LDLR protein in PCSK9 KO *versus* WT mice translate into an equivalent increase of LDLR protein at the hepatocyte cell surface in male, but not female mice (Fig. 1A) [19]. Similarly, liver cryosections of ovariectomized KO females supplemented with placebo (OvxP) presented a typical KO male pattern, while those supplemented with E2 (OvxE2) showed female-like surface labeling similar to WT (Fig. 1A), thereby indicating that E2 can negatively regulate LDLR surface density. We observed the same E2-regulation of cell surface LDLR density in another PCSK9 KO model (Supplementary Fig. S1) [18]. Note that protein levels analyzed by Western blot were insensitive to LDLR cell surface levels. In this context, several studies in cells, including ours [20], revealed that full length LDLR is essentially localized in the Golgi apparatus and in endosomes, and that cell surface LDLR only represents a small fraction of total LDLR (<5%).

A single E2 injection in PCSK9 KO Ovx females reduced surface LDLR labeling by 64% after 24h (Supplementary Fig. S2). Surface LDLR levels were back to their pre-treatment levels after 48h showing that the E2 effect was transitory. E2 injection in PCSK9 KO males also led to a marked drop in LDLR labeling 24h post-injection (Fig. 1B). This effect was detectable after >12h, indicating that E2-mediated LDLR decrease at the cell surface is a slow process. mRNA or protein LDLR levels remained unchanged (Supplementary Fig. S3).

In the classical pathway, cell-permeable estrogen binds cytoplasmic estrogen receptors alpha (ERα) or beta (ERβ), inducing their dimerization and translocation into the nucleus where they bind estrogen-responsive DNA elements (long-term effect). Estrogens also exert rapid effects via palmitoylated ERα or Gper1, another estrogen receptor [21]. The contribution of estrogen

receptors and/or Gper1 in the regulation of surface LDLR density was evaluated by testing E2, the ERα-specific agonist propyl pyrazole trisphenol (PPT) or the Gper1-specific agonist G-1 in PCSK9 KO Ovx females. Mice were euthanized 24h post-injection. Higher body weights in Ovx mice and loss or recovery of uterus weight were monitored as markers of successful treatment (Supplementary Fig. S4). LDLR labeling was 3-fold higher in vehicle-treated Ovx than sham-operated females (Fig. 2A). Both E2 and PPT treatments restored the typically low LDLR surface labeling observed in PCSK9 KO female mice, whereas G-1 had no effect (Fig. 2A). Changes in surface LDLR were not caused by modifications in LDLR mRNA levels in the liver (Supplementary Fig. S4A). We next analyzed the effect of inhibition of endogenous estrogen receptor activity in intact PCSK9 KO females (Fig. 2B). ERα/ERβ inhibition by ICI 182,780 reproduced 79% of the Ovx effect on LDLR labeling, while the Gper1 inhibitor G15 had no significant effect. As above, no LDLR mRNA change was observed (Supplementary Fig. S4B). Altogether, these data demonstrate that E2 reduces the cell surface density of the LDLR via ERα.

3.2. Female PCSK9 KO mice shed excess LDLR from hepatocytes

ADAM10 and ADAM17/TACE (TNFα-converting enzyme) are canonical sheddases of the a-disintegrin-and-metalloproteinase (ADAM) family. Because LDLR was shown to be shed by ADAM17 in bone marrow-derived monocytic cells [22] or by ADAM10 in neurons [23], we measured plasma sLDLR by ELISA in our mouse models. WT male and female mice presented similar levels of sLDLR (~150 ng/mL), whereas PCSK9 KO mice lacking (male; OvxP) or exposed to (female; OvxE2) estrogen had ~2- and 4-fold higher levels of sLDLR, respectively (Fig. 3A). Similar data were obtained in liver-specific PCSK9 KO mice as well as WT mice treated with alirocumab [13], a mAb neutralizing the LDLR binding of circulating PCSK9 (Supplementary Fig. S5). Thus, the absence of PCSK9 secreted from hepatocytes leads to LDLR accumulation at the cell surface in male livers only, likely due to lower shedding. To test the impact of E2 on LDLR shedding, WT and KO male mice received a single E2 injection and sLDLR levels were assessed for 28 hours. E2 had no effect in WT males but induced a transient >3-fold increase of sLDLR ~20 hours post-injection in KO male mice (Fig. 3B). In a second experiment, a subgroup of E2-injected KO males underwent a second E2 injection 24 hours after

the first one, and exhibited the same sLDLR response, indicating that surface LDLR levels were rapidly replenished (Supplementary Fig. S6). E2 triggered a similar peak of sLDLR in Ovx KO females (Supplementary Fig. S7A). Thus, E2 stimulates LDLR shedding in male PCSK9-deficient mice.

Acute systemic in vivo inhibition of metalloproteases is scarcely reported in the literature. First, we tested the general metalloprotease inhibitor BB-94 (Fig. 3C). In KO female mice, this resulted 4 hours after injection in a transient 86% drop in sLDLR. In WT females, BB-94 had a slower effect with a 66% reduction at 8 hours. Because many shedding events occur through cleavage by ADAM10 and 17 [24], we tested the effect of ZLDI-8, a novel inhibitor of ADAM17 and potentially additional metalloproteases (Fig. 4A) [25,26]. sLDLR levels were modestly affected in WT mice and PCSK9 KO male mice, but transitorily dropped to WT levels 8 hours post-injection in PCSK9 KO female mice. In agreement, ZLDI-8 specifically inhibited LDLR shedding in females, but not males treated with alirocumab (Supplementary Fig. S5D). In both experiments, ZLDI-8 reduced sLDLR levels back to basal WT female levels, suggesting that a ZLDI-8-sensitive sheddase, likely ADAM10 and/or ADAM17, is specifically active in PCSK9 KO females. In the presence of ZLDI-8, the LDLR continuously accumulates over time at the cell surface as it is no longer shed, leading to an impressive time-dependent increase of total LDLR at 16 hours (+81%; Fig. 4B). In parallel, LDLR staining of liver cryosections were ~2-fold increased, with no change in LDLR mRNA levels (Fig. 4C to E). ZLDI-8 also triggered a drop in sLDLR levels in sham-operated PCSK9 KO mice, but not Ovx ones (Supplementary Fig. S7B). Thus, in the absence of PCSK9 and presence of estrogen, a ZLDI-8-sensitive sheddase prevents LDLR accumulation in the liver. Neither ADAM17 nor ADAM10 mRNA levels, whose expression is higher in female mice and enhanced by E2 (up to 62%), were affected by genotype or ZLDI-8 treatment (Supplementary Fig. S8). Interestingly, even upon increasing ZLDI-8 concentration up to 25 mg/kg (*data not shown*), shedding inhibition was restricted to the enhanced portion of sLDLR resulting from the loss of PCSK9 in female mice, suggesting that the metalloprotease responsible for the E2-dependent shedding differs from the one(s) responsible for basal LDLR shedding. Notably, the maximal inhibition occurred after 8 hours at all concentrations, suggesting that ZLDI-8 has different inhibitory kinetics or selectivity than BB-94, which achieved a maximal effect after 4 hours (Figs. 3C and 4A).

3.3. PCSK9 KO male mice exhibit reduced intra-hepatic cholesterol contents

Since excess LDLR is efficiently shed from female hepatocytes, but not male ones, we hypothesized that their cholesterol content differs since high surface LDLR levels usually reflect an increased need for cholesterol. In plasma, a similar ~40% total cholesterol reduction was observed in KO male and female mice as compared to WT mice (Fig. 5A). In contrast, liver cholesterol levels were 30% and 22% lower in PCSK9 KO male and OvxP mice but were unchanged in PCSK9 KO female or OvxE2 livers (Fig. 5B). Thus, the lowest cholesterol content was observed in mice showing the strongest cell surface density of the LDLR. To our surprise, reduced cholesterol in male or OvxP livers did not result in the activation of the cholesterogenic SREBP-2 pathway. HMG-CoA reductase and LDLR mRNA levels were similar in WT and KO male mice or WT and KO OvxP female mice (Fig. 5C). To test whether LDLR shedding was induced by cholesterol, we orally administrated male mice with saline or mevalonate. The latter raised total cholesterol levels in KO livers by 2-fold and produced a remarkable 3-fold increase in sLDLR levels (Fig. 5D). A standard laboratory diet enriched in cholesterol produced in two weeks an even stronger effect with 3- and 5-fold higher levels of liver cholesterol and sLDLR, respectively (Supplementary Fig. S9).

Since E2 stimulates liver cholesterogenesis [27] and favors LDLR shedding via ERα (Fig. 2), we tested the capacity of E2 to simultaneously increase cholesterol and sLDLR levels. PCSK9 KO male mice were fed a regular diet supplemented or not with lovastatin, an HMG-CoA reductase inhibitor that prevents cholesterol synthesis, thereby activating SREBP-2. Indeed, lovastatin enhanced SREBP-2, HMG-CoA reductase and LDLR transcripts by 3-, 7-, and 1.5-fold, respectively (Supplementary Fig. S10A). Lovastatin further reduced plasma and intra-hepatic cholesterol levels by 40% and 50%, and led to ≥3-fold higher sLDLR levels (Supplementary Fig. S10B and C). The latter are explained by higher LDLR mRNA levels, but may also be due to a longer cell surface residence time of the LDLR. PCSK9 KO male mice exhibit 80% lower LDL levels. An additional 40% reduction in plasma cholesterol may further reduce LDLR internalization and enhance its shedding. Importantly, we show that this extra-fraction of sLDLR remained insensitive to ZLDI-8, in agreement with low liver cholesterol levels (Supplementary Fig. S10B and C). Finally, E2 injection in these mice produced similar net effects on plasma cholesterol and sLDLR levels (Fig. 5E and F). In both conditions, a peak

corresponding to an additional 0.7 μg/mL of sLDLR was produced 22 hours post-injection (Fig. 5F). Altogether, these data point at the existence of a cholesterol-dependent shedding that cannot take place in male mice lacking PCSK9 because of their low intra-hepatic cholesterol content.

3.4. Proliferating hepatocytes in PCSK9 KO Ovx mice exhibit a G2/M cell cycle arrest

We undertook a transcriptomic analysis of E2-mediated transcriptional effects in OvxP and OvxE2 livers from WT and KO female mice. Upon E2 treatment, 736 and 80 differentially expressed genes (DEGs) were identified in WT and KO Ovx mice, respectively (Fig. 6A). Surprisingly, only 2% of the WT DEGs (15 genes) were similarly regulated by E2 in WT and KO livers (Fig. 6). Thus, the loss of PCSK9 blunted the regulation of 98% of the WT DEGs by E2, even if ERα is clearly present in all samples (Supplementary Fig. S11).

Even though the expression of *Srebf2*, *Ldlr* or the 22 cholesterogenic genes was globally sensitive to female sex or E2 (+12 to 65%; Supplementary Fig. S12), none of these genes exhibited a significant fold-change >1.5. Instead, we identified among the 80 DEGs in KO Ovx mice a functional network of 54 proteins related to the G2/M transition of the cell cycle (Fig. 6B and Supplementary Figs. S13 and S14). During this transition, chromosomal centromeres connect with spindle microtubules via kinetochores before segregation, while material is recruited to the cleavage furrow to prepare the final separation of the mother cell into daughter cells. In WT samples, the 54 genes were upregulated by E2 (+48% in average; Fig. 6B and C) in agreement with the pro-proliferative effect of E2 on hepatocytes in vivo [28,29]. In KO samples, the average expression of the 54 genes was 116% higher than in WT ones, but reverted to OvxP WT levels by E2 supplementation. This expression pattern was verified by QPCR for 18 genes, both in intact and Ovx mice (Supplementary Fig. S15). The promoter regions of the 54 genes do not share binding sites for ERα or ERα co-factors, suggesting that they are not directly regulated by E2. In contrast, 35 of the 54 genes are regulated by the transcription factor FOXM1 (Supplementary Fig. S16), in agreement with its capacity to activate ~70% of the genes implicated in the G2/M transition [30-32].

Our data indicate that the G2/M transition is delayed in cycling hepatocytes of PCSK9 KO male mice because of critically low cholesterol, and that this transition is rescued by E2 supplementation. First, although G2/M represents 20% of the cell cycle in duration, only G2/M

transition-specific transcripts were found at high levels in KO OvxP livers, suggesting that this accumulation is caused by cell cycle arrest rather than increased proliferation. Second, FOXM1 was reported to remain active in cells arrested in G2, explaining the sustained levels of the 54 gene-set expression [33]. Third, while E2 has a pro-proliferative effect, it reduced G2/M transcripts by 66% in KO livers, indicating that it rather normalizes G2/M mRNA levels. Finally, we have reported previously that liver regeneration was delayed in PCSK9 KO males that underwent partial hepatectomy, a phenotype rescued by high cholesterol feeding [6].

4. Discussion

In this study, we analyzed how male and female hepatocytes differentially respond to excess LDLR generated by the absence of PCSK9. We discovered that female mice actively shed LDLR in the plasma, thus rationalizing the absence of cell surface accumulation of the LDLR (Fig. 7). The effect of E2 in PCSK9 KO male mice is drastic: in ~20 hours, it reduces LDLR cell surface labeling to WT levels and concomitantly induces a 3-fold increase in circulating sLDLR in an ERα-dependent manner.

LDLR shedding in PCSK9 KO female mice was transiently inhibited by a general metalloprotease inhibitor. Both ADAM17 and ADAM10 were reported to shed the LDLR in bone marrow-derived cells or primary neurons, respectively [22,23], and ADAM17 was recently shown to shed the closely related VLDLR [34]. We thus tested ZLDI-8, which has been reported an ADAM17-specific inhibitor [25,26,35]. Independently of its concentration, it lowered sLDLR levels in PCSK9 KO female plasma down to WT ones. Notably, inhibition of this female-specific shedding generates a further 80% accumulation of the LDLR in the liver within a few hours (Fig. 4). ZLDI-8 had no effect on sLDLR levels in WT mice or KO male mice. Although we cannot exclude that ZLDI-8 also targets ADAM10 [36], as most hydroxamates are not highly selective for ADAM10 or ADAM17, our data suggest that the ZLDI-8-inhibited sheddase differs from the one(s) shedding LDLR in WT or KO male mice. Such basal shedding is 2-fold higher in KO male mice than in WT mice. During our study, Alabi and colleagues reported that sLDLR was reduced by 67% upon *Mmp14* (MT1-MMP) gene inactivation in the mouse liver [37]. This

suggests that MMP14 and/or other metalloproteases can shed more LDLR upon an increased flux of the receptor towards the hepatocyte cell surface.

E2 reduces the cell surface density of the LDLR in male or Ovx mice lacking PCSK9 via a transcriptional effect mediated by ERα (Fig. 2) that cannot be explained by a differential regulation of ADAM17 or ADAM10 expression in WT and KO mice (Supplementary Fig. S8). Instead, we hypothesized that the female-specific shedding activity depends on the membrane cholesterol content, which is lower in PCSK9 KO male and OvxP livers (-30% and -22%, respectively; Fig. 5). Indeed, mevalonate or high cholesterol feeding that raises intra-hepatic cholesterol also elevated plasma sLDLR levels of KO male mice (Fig. 5 and Supplementary Fig. S10). E2 was shown to strongly stimulate via ERα cholesterol synthesis in the liver as estimated by the rate of incorporation of ^{3}H-labeled water into sterols [27]. In our study, E2 increases cholesterol levels in PCSK9 KO male mice in ~12 hours. Within a few more hours, excess LDLR is shed. Shedding activities were reported to be sensitive to membrane cholesterol content or distribution [38]. Different from ADAM10, ADAM17 is segregated to lipid rafts, together with furin that contributes to its activation in the trans-Golgi network [39]. In the liver, ADAM17 was shown to cleave TNFα in cholesterol-enriched domains [40]. Caveolin deficiency or cyclodextrin treatment of primary hepatocytes also inhibited TGFβ1 shedding by ADAM17 [41]. Interestingly, the LXR-IDOL degradation pathway of LDLR and VLDLR was localized in lipid rafts [42]. It remains to be determined where the excess LDLR is targeted in PCSK9 KO female, but not male hepatocytes to favor its shedding.

This study reveals that despite 3- to 4-fold higher levels of cell surface LDLR, KO male or Ovx mice cannot replenish their liver cholesterol content, likely due to 80% lower levels of circulating LDL in PCSK9 KO mice. Surprisingly, these mice do not stimulate their SREBP-2 pathway (Supplementary Fig. S12). Cholesterol trafficking from endosomes to the plasma membrane and then to the endoplasmic reticulum (ER) may be modified in the absence of PCSK9 [43,44]. Whether the recruitment of the ER-anchored Aster proteins (*Gramd* genes) at contact sites with lysosomal or plasma membranes differs and favors the non-vesicular transfer of cholesterol to the ER remains to be determined [45-47]. Alternatively, phosphatidylserine distribution may be altered. Aster proteins bind this phospholipid in the inner leaflet of the plasma membrane, while its presence on the outer leaflet stimulates ADAM10 and 17 activity

[48-51]. Future analysis of how the absence of PCSK9 disrupts the sensing and/or regulatory mechanisms adjusting cholesterol synthesis through SREBP-2 should be extremely interesting.

The lack of cholesterol that hampers LDLR shedding in PCSK9 KO male mice also affects hepatocyte proliferation. Cytokinesis requires a massive cholesterol input to form a membranous barrier between daughter cells, and the existence of a G2 checkpoint was reported to be activated by cholesterol deprivation through CDK1 inactivation in synchronized cells [52,53]. Thanks to its ERα-mediated pro-proliferation impact, E2 treatment of KO Ovx mice reverted to WT levels the expression of 54 genes related to G2/M transition, indicating that the transient G2/M arrest is released. In this context, it will be of interest to verify whether female mice are protected from delayed hepatocyte proliferation and liver necrotic areas, two hallmarks of regenerating livers in PCSK9 KO male mice that are rescued upon cholesterol feeding [6].

Another surprising observation is that the loss of PCSK9 leads to a dramatic loss of E2 regulation that cannot be explained by the loss of ERα mRNA or protein (Supplementary Fig. S7): only 2% of the 736 genes regulated by E2 supplementation in WT Ovx females were similarly regulated in PCSK9 KO Ovx females. Also, the hypothesis of increased E2 neutralization via sulfation, which prevents ERα binding, or E2 conversion to estrone seems unlikely as the pellets generate an average 15-fold excess in circulating E2 compared to physiological levels. Whether ERα trafficking between the cytosol and nucleus or its association with membranes (palmitoylation and/or interaction with caveolin-1) is modified in the absence of PCSK9, making ERα less available for nuclear regulation, remains to be analyzed.

5. Conclusion

In this study, we showed that female mice lacking PCSK9 exhibit an alternative pathway to control surface LDLR density in the liver. This E2-driven process may respond to female-specific needs. Lower levels of cell surface LDLR in the liver may favor lipoprotein uptake by peripheral tissues or growing embryos. In this context, we previously observed that the loss of PCSK9 leads to higher surface levels of the LDLR in enterocytes and VLDLR in visceral adipose tissue of female, but not male mice [19]. Interestingly, *PCSK9* pseudogenization in the large group of placental mammals Laurasiatheria occurred repeatedly, indicating that alteration in their cholesterol metabolism made them more susceptible to lose PCSK9 [54]. Therefore, in

species lacking PCSK9, including pigs, bovines, camels, whales, bats, cats, dogs, bears and horses, it would be interesting to evaluate the functional relevance and metabolic consequences of E2-mediated shedding of liver surface LDLR.

Even though women benefit from PCSK9 lowering therapy as well as men, they often exhibit a 15-20% lower LDL-C reduction when treated with PCSK9 mAbs [14-17]. Because this may reflect higher LDLR shedding in women lacking PCSK9, we measured sLDLR levels in the plasma of men and pre-menopausal women that receive PCSK9 mAbs and matched for age (Supplementary Fig. S13). Pre-menopausal women exhibited 1.8-fold higher sLDLR, thus supporting the translational relevance of our mouse data. The analysis of the plasma of loss-of-function women should be highly informative. But these latter samples are rare and difficult to obtain. The physiological role(s) of circulating sLDLR is still a matter of debate [55]. How lower surface LDLR levels or higher circulating sLDLR affect lipoprotein clearance, and possibly other functions of the receptor, as pathogen lipid clearance or inflammation [13], will require further studies in patients.

Credit authorship contribution statement

AP and NGS conceived, designed and funded the study. AR, DG and SL contributed to experimental design. AR, DG, SL, AC, JM, and TS conducted and analyzed experiments. DG performed statistical analyses. MP and SB provided human plasma. RM, BC, CLM, MK, NGS and AP contributed to the experimental design and analyzed the data. AP wrote and edited the manuscript and all authors read and approved its final version.

Declaration od competing interest

The authors declare that the research was conducted in the absence of any commercial or financial relationships that could be construed as a potential conflict of interest.

Acknowledgments

This study was supported by the Fondation Leducq Transatlantic Network of Excellence in Cardiovascular Research 13CVD03, the Canadian Institutes of Health Research (CIHR) Foundation Catalyst Grant program, Sex and variables 145572, CIHR Foundation grant 148363, and CIHR Canada Chair 950-231335.
We thank Suzie Riverin for animal care, François Couderc and Myriam Rondeau for genotyping, Odile Neyret, Virginie Caldéron and Caroline Grou for RNA sequencing and analyses. We are particularly grateful to Carl P. Blobel for his insights and helpful discussions.

Credit authorship contribution statement

AP and NGS conceived, designed and funded the study. AR, DG and SL contributed to experimental design. AR, DG, SL, AC, JM, and TS conducted and analyzed experiments. DG performed statistical analyses. MP and SB provided human plasma. RM, BC, CLM, MK, NGS and AP contributed to the experimental design and analyzed the data. AP wrote and edited the manuscript and all authors read and approved its final version.

Declaration od competing interest

The authors declare that the research was conducted in the absence of any commercial or financial relationships that could be construed as a potential conflict of interest.

Acknowledgments

This study was supported by the Fondation Leducq Transatlantic Network of Excellence in Cardiovascular Research 13CVD03, the Canadian Institutes of Health Research (CIHR) Foundation Catalyst Grant program, Sex and variables 145572, CIHR Foundation grant 148363, and CIHR Canada Chair 950-231335.
We thank Suzie Riverin for animal care, François Couderc and Myriam Rondeau for genotyping, Odile Neyret, Virginie Caldéron and Caroline Grou for RNA sequencing and analyses. We are particularly grateful to Carl P. Blobel for his insights and helpful discussions.

References

[1] M.S. Brown, A. Radhakrishnan, J.L. Goldstein, Retrospective on Cholesterol Homeostasis: The Central Role of Scap, Annu Rev Biochem, 87 (2018) 783-807.
[2] N.G. Seidah, A. Prat, The biology and therapeutic targeting of the proprotein convertases, Nat Rev Drug Discov, 11 (2012) 367-383.
[3] M.C. McNutt, T.A. Lagace, J.D. Horton, Catalytic activity is not required for secreted PCSK9 to reduce low density lipoprotein receptors in HepG2 cells, Journal of Biological Chemistry, 282 (2007) 20799-20803.
[4] N.G. Seidah, S. Benjannet, L. Wickham, J. Marcinkiewicz, S.B. Jasmin, S. Stifani, A. Basak, A. Prat, M. Chretien, The secretory proprotein convertase neural apoptosis-regulated convertase 1 (NARC-1): liver regeneration and neuronal differentiation, Proceedings of the National Academy of Sciences of the United States of America, 100 (2003) 928-933.
[5] M.L. Peyot, A. Roubtsova, R. Lussier, A. Chamberland, R. Essalmani, S.R. Murthy Madiraju, N.G. Seidah, M. Prentki, A. Prat, Substantial PCSK9 inactivation in β-cells does not modify glucose homeostasis or insulin secretion in mice, Biochim Biophys Acta Mol Cell Biol Lipids, 1866 (2021) 158968.
[6] A. Zaid, A. Roubtsova, R. Essalmani, J. Marcinkiewicz, A. Chamberland, J. Hamelin, M. Tremblay, H. Jacques, W. Jin, J. Davignon, N.G. Seidah, A. Prat, Proprotein convertase subtilisin/kexin type 9 (PCSK9): Hepatocyte-specific low-density lipoprotein receptor degradation and critical role in mouse liver regeneration, Hepatology, 48 (2008) 646-654.
[7] T.A. Lagace, D.E. Curtis, R. Garuti, M.C. McNutt, S.W. Park, H.B. Prather, N.N. Anderson, Y.K. Ho, R.E. Hammer, J.D. Horton, Secreted PCSK9 decreases the number of LDL receptors in hepatocytes and inlivers of parabiotic mice, Journal of Clinical Investigation, 116 (2006) 2995-3005.
[8] K.N. Maxwell, J.L. Breslow, Adenoviral-mediated expression of Pcsk9 in mice results in a low-density lipoprotein receptor knockout phenotype, Proceedings of the National Academy of Sciences of the United States of America, 101 (2004) 7100-7105.
[9] K.N. Maxwell, E.A. Fisher, J.L. Breslow, Overexpression of PCSK9 accelerates the degradation of the LDLR in a post-endoplasmic reticulum compartment, Proceedings of the National Academy of Sciences of the United States of America, 102 (2005) 2069-2074.
[10] M. Abifadel, M. Varret, J.P. Rabes, D. Allard, K. Ouguerram, M. Devillers, C. Cruaud, S. Benjannet, L. Wickham, D. Erlich, A. Derre, L. Villeger, M. Farnier, I. Beucler, E. Bruckert, J. Chambaz, B. Chanu, J.M. Lecerf, G. Luc, P. Moulin, J. Weissenbach, A. Prat, M. Krempf, C. Junien, N.G. Seidah, C. Boileau, Mutations in PCSK9 cause autosomal dominant hypercholesterolemia, Nature Genetics, 34 (2003) 154-156.
[11] J. Cohen, A. Pertsemlidis, I.K. Kotowski, R. Graham, C.K. Garcia, H.H. Hobbs, Low LDL cholesterol in individuals of African descent resulting from frequent nonsense mutations in PCSK9, Nature Genetics, 37 (2005) 161.
[12] J.C. Chan, D.E. Piper, Q. Cao, D. Liu, C. King, W. Wang, J. Tang, Q. Liu, J. Higbee, Z. Xia, Y. Di, S. Shetterly, Z. Arimura, H. Salomonis, W.G. Romanow, S.T. Thibault, R. Zhang, P. Cao, X.P. Yang, T. Yu, M. Lu, M.W. Retter, G. Kwon, K. Henne, O. Pan, M.M. Tsai, B. Fuchslocher, E. Yang, L. Zhou, K.J. Lee, M. Daris, J. Sheng, Y. Wang, W.D. Shen, W.C. Yeh, M. Emery, N.P. Walker, B. Shan, M. Schwarz, S.M. Jackson, A proprotein convertase subtilisin/kexin type 9 neutralizing antibody reduces serum cholesterol in mice and nonhuman primates, Proceedings of the National Academy of Sciences of the United States of America, 106 (2009) 9820-9825.
[13] N.G. Seidah, A. Prat, The multifaceted biology of PCSK9, Endocr Rev, 43 (2022) 558-582.
[14] A. Cordero, M.R. Fernández Del Olmo, G.A. Cortez Quiroga, C. Romero-Menor, L. Fácila, J. Seijas-Amigo, A. Fornovi, J.R. Murillo, M. Rodríguez-Mañero, M.C. Bello Mora, A. Valle, S. Miriam, R.F. Pamias, J. Bañeras, P.B. García, M.M. Clemente Lorenzo, S. Sánchez-Alvarez, L. López-Rodríguez, J.R. González-Juanatey, Sex Differences in Low-Density Lipoprotein Cholesterol Reduction With

PCSK9 Inhibitors in Real-world Patients: The LIPID-REAL Registry, J Cardiovasc Pharmacol, 79 (2022) 523-529.
[15] P. Sever, I. Gouni-Berthold, A. Keech, R. Giugliano, T.R. Pedersen, K. Im, H. Wang, B. Knusel, M.S. Sabatine, M.L. O'Donoghue, LDL-cholesterol lowering with evolocumab, and outcomes according to age and sex in patients in the FOURIER Trial, Eur J Prev Cardiol, 28 (2021) 805-812.
[16] J.G. Robinson, M. Farnier, M. Krempf, J. Bergeron, G. Luc, M. Averna, E.S. Stroes, G. Langslet, F.J. Raal, S.M. El, M.J. Koren, N.E. Lepor, C. Lorenzato, R. Pordy, U. Chaudhari, J.J. Kastelein, Efficacy and safety of alirocumab in reducing lipids and cardiovascular events, N. Engl. J. Med. , 372 (2015) 1489-1499.
[17] J. Golden, M. Roberts, Clinical Briefing Document, FDA Endocrinologic and Metabolic Drugs Advisory Committee, Alirocumab (praluent) in, 2015.
[18] S. Rashid, D.E. Curtis, R. Garuti, N.N. Anderson, Y. Bashmakov, Y.K. Ho, R.E. Hammer, Y.A. Moon, J.D. Horton, Decreased plasma cholesterol and hypersensitivity to statins in mice lacking Pcsk9, Proceedings of the National Academy of Sciences of the United States of America, 102 (2005) 5374-5379.
[19] A. Roubtsova, A. Chamberland, J. Marcinkiewicz, R. Essalmani, A. Fazel, J.J. Bergeron, N.G. Seidah, A. Prat, PCSK9 deficiency unmasks a sex/tissue-specific subcellular distribution of the LDL and VLDL receptors in mice, Journal of Lipid Research, 56 (2015) 2133-2142.
[20] D. Susan-Resiga, E. Girard, R.S. Kiss, R. Essalmani, J. Hamelin, M.C. Asselin, Z. Awan, C. Butkinaree, A. Fleury, A. Soldera, Y.L. Dory, A. Baass, N.G. Seidah, The Proprotein Convertase Subtilisin/Kexin Type 9-resistant R410S Low Density Lipoprotein Receptor Mutation: A novel mechanism causing familial hypercholesterolemia, J Biol Chem, 292 (2017) 1573-1590.
[21] G. Sharma, F. Mauvais-Jarvis, E.R. Prossnitz, Roles of G protein-coupled estrogen receptor GPER in metabolic regulation, J Steroid Biochem Mol Biol, 176 (2018) 31-37.
[22] L. Guo, J.R. Eisenman, R.M. Mahimkar, J.J. Peschon, R.J. Paxton, R.A. Black, R.S. Johnson, A proteomic approach for the identification of cell-surface proteins shed by metalloproteases, Mol Cell Proteomics, 1 (2002) 30-36.
[23] P.H. Kuhn, A.V. Colombo, B. Schusser, D. Dreymueller, S. Wetzel, U. Schepers, J. Herber, A. Ludwig, E. Kremmer, D. Montag, U. Müller, M. Schweizer, P. Saftig, S. Bräse, S.F. Lichtenthaler, Systematic substrate identification indicates a central role for the metalloprotease ADAM10 in axon targeting and synapse function, Elife, 5 (2016).
[24] T. Kawai, K.J. Elliott, R. Scalia, S. Eguchi, Contribution of ADAM17 and related ADAMs in cardiovascular diseases, Cell Mol Life Sci, 78 (2021) 4161-4187.
[25] H.Y. Lu, Y.X. Zu, X.W. Jiang, X.T. Sun, T.Y. Liu, R.L. Li, Q. Wu, Y.S. Zhang, Q.C. Zhao, Novel ADAM-17 inhibitor ZLDI-8 inhibits the proliferation and metastasis of chemo-resistant non-small-cell lung cancer by reversing Notch and epithelial mesenchymal transition in vitro and in vivo, Pharmacol Res, 148 (2019) 104406.
[26] D.D. Li, C.H. Zhao, H.W. Ding, Q. Wu, T.S. Ren, J. Wang, C.Q. Chen, Q.C. Zhao, A novel inhibitor of ADAM17 sensitizes colorectal cancer cells to 5-Fluorouracil by reversing Notch and epithelial-mesenchymal transition in vitro and in vivo, Cell Prolif, 51 (2018) e12480.
[27] H.H. Wang, N.H. Afdhal, D.Q. Wang, Overexpression of estrogen receptor alpha increases hepatic cholesterogenesis, leading to biliary hypersecretion in mice, J Lipid Res, 47 (2006) 778-786.
[28] Y. Tsugawa, M. Natori, H. Handa, T. Imai, Estradiol accelerates liver regeneration through estrogen receptor α, Clin Exp Gastroenterol, 12 (2019) 331-336.
[29] M. Umeda, M. Hiramoto, T. Imai, Partial hepatectomy induces delayed hepatocyte proliferation and normal liver regeneration in ovariectomized mice, Clin Exp Gastroenterol, 8 (2015) 175-182.
[30] J. Laoukili, M.R. Kooistra, A. Brás, J. Kauw, R.M. Kerkhoven, A. Morrison, H. Clevers, R.H. Medema, FoxM1 is required for execution of the mitotic programme and chromosome stability, Nat Cell Biol, 7 (2005) 126-136.
[31] S. Sadasivam, S. Duan, J.A. DeCaprio, The MuvB complex sequentially recruits B-Myb and FoxM1 to promote mitotic gene expression, Genes Dev, 26 (2012) 474-489.

[32] G.D. Grant, L. Brooks, 3rd, X. Zhang, J.M. Mahoney, V. Martyanov, T.A. Wood, G. Sherlock, C. Cheng, M.L. Whitfield, Identification of cell cycle-regulated genes periodically expressed in U2OS cells and their regulation by FOXM1 and E2F transcription factors, Mol Biol Cell, 24 (2013) 3634-3650.
[33] M. Alvarez-Fernández, V.A. Halim, L. Krenning, M. Aprelia, S. Mohammed, A.J. Heck, R.H. Medema, Recovery from a DNA-damage-induced G2 arrest requires Cdk-dependent activation of FoxM1, EMBO Rep, 11 (2010) 452-458.
[34] X. Ma, Y. Takahashi, W. Wu, W. Liang, J. Chen, D. Chakraborty, Y. Li, Y. Du, S. Benyajati, J.X. Ma, ADAM17 mediates ectodomain shedding of the soluble VLDL receptor fragment in the retinal epithelium, J Biol Chem, 297 (2021) 101185.
[35] Y. Zhang, D. Li, Q. Jiang, S. Cao, H. Sun, Y. Chai, X. Li, T. Ren, R. Yang, F. Feng, B.A. Li, Q. Zhao, Novel ADAM-17 inhibitor ZLDI-8 enhances the in vitro and in vivo chemotherapeutic effects of Sorafenib on hepatocellular carcinoma cells, Cell Death Dis, 9 (2018) 743.
[36] R.O. Alabi, J. Lora, A.B. Celen, T. Maretzky, C.P. Blobel, Analysis of the Conditions That Affect the Selective Processing of Endogenous Notch1 by ADAM10 and ADAM17, Int J Mol Sci, 22 (2021).
[37] A. Alabi, X.D. Xia, H.M. Gu, F. Wang, S.J. Deng, N. Yang, A. Adijiang, D.N. Douglas, N.M. Kneteman, Y. Xue, L. Chen, S. Qin, G. Wang, D.W. Zhang, Membrane type 1 matrix metalloproteinase promotes LDL receptor shedding and accelerates the development of atherosclerosis, Nat Commun, 12 (2021) 1889.
[38] K. Reiss, S. Bhakdi, The plasma membrane: Penultimate regulator of ADAM sheddase function, Biochim Biophys Acta Mol Cell Res, 1864 (2017) 2082-2087.
[39] J. Schlöndorff, J.D. Becherer, C.P. Blobel, Intracellular maturation and localization of the tumour necrosis factor alpha convertase (TACE), Biochem J, 347 Pt 1 (2000) 131-138.
[40] E. Tellier, M. Canault, L. Rebsomen, B. Bonardo, I. Juhan-Vague, G. Nalbone, F. Peiretti, The shedding activity of ADAM17 is sequestered in lipid rafts, Exp Cell Res, 312 (2006) 3969-3980.
[41] J. Moreno-Càceres, L. Caja, J. Mainez, R. Mayoral, P. Martín-Sanz, R. Moreno-Vicente, M. Del Pozo, S. Dooley, G. Egea, I. Fabregat, Caveolin-1 is required for TGF-β-induced transactivation of the EGF receptor pathway in hepatocytes through the activation of the metalloprotease TACE/ADAM17, Cell Death Dis, 5 (2014) e1326.
[42] V. Sorrentino, J.K. Nelson, E. Maspero, A.R.A. Marques, L. Scheer, S. Polo, N. Zelcer, The LXR-IDOL axis defines a clathrin-, caveolae-, and dynamin-independent endocytic route for LDLR internalization and lysosomal degradation, J Lipid Res, 54 (2013) 2174-2184.
[43] A.D. Sniderman, Y. Qi, C.I. Ma, R.H. Wang, M. Naples, C. Baker, J. Zhang, K. Adeli, R.S. Kiss, Hepatic cholesterol homeostasis: is the low-density lipoprotein pathway a regulatory or a shunt pathway?, Arterioscler Thromb Vasc Biol, 33 (2013) 2481-2490.
[44] R.E. Infante, A. Radhakrishnan, Continuous transport of a small fraction of plasma membrane cholesterol to endoplasmic reticulum regulates total cellular cholesterol, Elife, 6 (2017).
[45] A. Ferrari, C. He, J.P. Kennelly, J. Sandhu, X. Xiao, X. Chi, H. Jiang, S.G. Young, P. Tontonoz, Aster Proteins Regulate the Accessible Cholesterol Pool in the Plasma Membrane, Mol Cell Biol, 40 (2020).
[46] T. Naito, Y. Saheki, GRAMD1-mediated accessible cholesterol sensing and transport, Biochim Biophys Acta Mol Cell Biol Lipids, 1866 (2021) 158957.
[47] D. Höglinger, T. Burgoyne, E. Sanchez-Heras, P. Hartwig, A. Colaco, J. Newton, C.E. Futter, S. Spiegel, F.M. Platt, E.R. Eden, NPC1 regulates ER contacts with endocytic organelles to mediate cholesterol egress, Nat Commun, 10 (2019) 4276.
[48] M.N. Trinh, M.S. Brown, J.L. Goldstein, J. Han, G. Vale, J.G. McDonald, J. Seemann, J.T. Mendell, F. Lu, Last step in the path of LDL cholesterol from lysosome to plasma membrane to ER is governed by phosphatidylserine, Proc Natl Acad Sci U S A, 117 (2020) 18521-18529.
[49] J. Sandhu, S. Li, L. Fairall, S.G. Pfisterer, J.E. Gurnett, X. Xiao, T.A. Weston, D. Vashi, A. Ferrari, J.L. Orozco, C.L. Hartman, D. Strugatsky, S.D. Lee, C. He, C. Hong, H. Jiang, L.A. Bentolila, A.T. Gatta, T.P. Levine, A. Ferng, R. Lee, D.A. Ford, S.G. Young, E. Ikonen, J.W.R. Schwabe, P. Tontonoz,

Aster Proteins Facilitate Nonvesicular Plasma Membrane to ER Cholesterol Transport in Mammalian Cells, Cell, 175 (2018) 514-529.e520.
[50] A. Sommer, F. Kordowski, J. Büch, T. Maretzky, A. Evers, J. Andrä, S. Düsterhöft, M. Michalek, I. Lorenzen, P. Somasundaram, A. Tholey, F.D. Sönnichsen, K. Kunzelmann, L. Heinbockel, C. Nehls, T. Gutsmann, J. Grötzinger, S. Bhakdi, K. Reiss, Phosphatidylserine exposure is required for ADAM17 sheddase function, Nat Commun, 7 (2016) 11523.
[51] F. Bleibaum, A. Sommer, M. Veit, B. Rabe, J. Andrä, K. Kunzelmann, C. Nehls, W. Correa, T. Gutsmann, J. Grötzinger, S. Bhakdi, K. Reiss, ADAM10 sheddase activation is controlled by cell membrane asymmetry, J Mol Cell Biol, 11 (2019) 979-993.
[52] J. Martínez-Botas, Y. Suárez, A.J. Ferruelo, D. Gómez-Coronado, M.A. Lasuncion, Cholesterol starvation decreases p34(cdc2) kinase activity and arrests the cell cycle at G2, Faseb j, 13 (1999) 1359-1370.
[53] Y. Suárez, C. Fernández, B. Ledo, A.J. Ferruelo, M. Martín, M.A. Vega, D. Gómez-Coronado, M.A. Lasunción, Differential effects of ergosterol and cholesterol on Cdk1 activation and SRE-driven transcription, Eur J Biochem, 269 (2002) 1761-1771.
[54] B. van Asch, L.F. Teixeira da Costa, Patterns and tempo of PCSK9 pseudogenizations suggest an ancient divergence in mammalian cholesterol homeostasis mechanisms, Genetica, 149 (2021) 1-19.
[55] J. Mayne, T.C. Ooi, L. Tepliakova, D. Seebun, K. Walker, D. Mohottalage, Z. Ning, H. Abujrad, M. Mbikay, H. Wassef, M. Chrétien, D. Figeys, Associations Between Soluble LDLR and Lipoproteins in a White Cohort and the Effect of PCSK9 Loss-of-Function, J Clin Endocrinol Metab, 103 (2018) 3486-3495.

Figure legends

Fig. 1. The cell surface density of the LDLR in the liver of PCSK9-deficient mice is reduced by estrogens. (A) LDLR staining of liver sections from PCSK9 WT and KO male and female mice, or OvxP and OvxE2 female mice was quantified (n=9-10 mice). (B) LDLR staining of liver sections from KO males that received a single injection of E2 was assessed during 24 hours (n=4-5 mice). Mean±SEM. *P* values were determined by using Kruskal-Wallis followed by Dunn's multiple comparisons test.

Fig. 2. E2 reduces LDLR density at the hepatocyte cell surface via ERα in PCSK9-deficient mice. (A) PCSK9-deficient female mice were sham-operated or ovariectomized (Ovx) and injected with vehicle (Veh), E2 (50 μg/kg) or the ERα and Gper1 agonists, PPT (2.5 mg/kg) and G-1 (50 mg/kg), respectively (n=7-8 mice). (B) Ovx or intact PCSK9-deficient mice were injected with Veh, ERα/ERβ inhibitor ICI 182,780 (daily injection of 10 mg/kg for 4 days) or Gper1 inhibitor G15 (0.25 mg/kg). All mice were analyzed 24h post-treatment (n=4-5 mice). LDLR labeling intensity was normalized to values for Ovx (A) or intact (B) mice treated with Veh. Mean±SEM. *P* were determined using Kruskal-Wallis test followed by Dunn's multiple comparisons test.

Fig. 3. Shedding of excess LDLR in PCSK9-deficient mice depends on estrogen and is achieved by metalloproteases. (A) Plasma levels of shed LDLR (sLDLR) were assessed in all mouse models and normalized to WT male levels. n=4-5 mice. (B) sLDLR was measured for 28h in WT and KO male mice after vehicle (Veh) or E2 injection (50 μg/kg; n=4-6 mice). (C) WT and KO female mice received an intraperitoneal injection of vehicle or the metalloprotease inhibitor BB-94 (12.5 mg/kg; n=4-5 mice). Mean±SEM were normalized to WT Veh value at t=0 and set to 1. *P* values were determined using Mann-Whitney *U* test (A; non parametric data) and 2-way ANOVA followed by Tukey's multiple comparisons test (B and C).

Fig. 4. Shedding of excess LDLR in PCSK9-deficient female mice is specifically inhibited by ZLDI-8. (A) sLDLR was assessed in WT and KO plasma after injection the ADAM17 inhibitor ZLDI-8 (10 mg/kg). (B-E) Liver LDLR protein, mRNA, and surface LDLR staining were analyzed (n=5-9 mice). Mean±SEM. *P* values were determined using 2-way ANOVA followed by Tukey's multiple comparisons test.

Fig. 5. PCSK9-deficient male and OvxP mice exhibit low liver cholesterol contents that are normalized by mevalonate feeding or E2, leading to excess LDLR shedding. (A) Plasma (n=5-14 mice) and (B) liver total cholesterol (n=8-10 mice) were measured. (C) Levels of transcripts encoding HMG-CoA reductase (*Hmgcr*), LDLR and PCSK9 were analyzed by QPCR in WT and KO intact or OvxP and OvxE2 mice. n=4-5 mice. (D) Liver cholesterol and sLDLR levels were stimulated in PCSK9 KO male mice after 9 days of gavage with saline (normalized values set to 1) or mevalonate (35 mg/kg/day; n=7-11 mice). (E) Plasma cholesterol and sLDLR levels were similarly upregulated by E2 in mice fed a regular diet supplemented or not with 0.2% lovastatin for 10 days (n=9-10 mice). Mean±SEM. *P* values were determined using Mann-Whitney *U* test (A and D), unpaired Student's t-test with Welch's correction (B), Kruskal-Wallis followed by

Dunn's multiple comparisons test (C), and 2-way ANOVA followed by Tukey's multiple comparisons test (E-F).

Fig. 6. Effect of E2 supplementation on the liver transcriptome of Ovx females. (A) The Venn diagram shows that 736 genes are regulated by E2 in WT Ovx livers, while 80 genes are regulated by E2 in KO livers (n=3). (B) Out of these 80 differently expressed genes (DEGs), STRING analysis identified a single cluster of proteins implicating 54 DEGs related to the cell cycle (Supplementary Fig. S14; FDR, false discovery rate). A box plot of the 54 DEGs normalized counts in WT and KO OvxP or OvxE2 livers is shown, and medians are compared. (C) The 80 DEGs are sorted by decreasing log2(E2/P) in KO livers (red bars). Corresponding WT log2(E2/P) values are shown in green. The 15 DEGs that are similarly upregulated by E2 in both WT and KO Ovx livers (Venn diagram) appear in a blue box. Squares point at the 54 DEGs and filled ones were confirmed by QPCR.

Fig. 7. Sex-specific consequences of the absence of PCSK9 on LDLR levels in mouse hepatocytes. In male and female WT mice (green box), only a portion of the LDLR is recycled back to the cell surface following LDL internalization. Indeed, circulating PCSK9 can bind cell surface LDLR and prevent its recycling by escorting it to lysosomes. In addition, a fraction of the cell surface LDLR is shed by metalloproteases (basal shedding). In PCSK9 KO mice, total liver LDLR protein levels are 4-fold higher, but cell surface LDLR levels differ in male (x 4) and female (x 2) mice. The absence of PCSK9 in male mice is associated with an increased LDLR basal shedding (x 2) and results in critically low liver cholesterol (left red box), leading to a delay in the G2/M transition of the cell cycle, a step known to be dependent on cholesterol. In contrast, female cholesterol levels are sustained by the cholesterogenic effect of 17β-estradiol (E2) mediated via the estrogen receptor alpha (ERα) and SREBP-2 activation (right red box). This results in a female-specific and cholesterol-dependent shedding by ADAM10/17 that doubles shed LDLR levels (sLDLR) in plasma. This cholesterol-dependent LDLR shedding may explain the 15-20% lower LDL-cholesterol reduction observed in women treated with PCSK9 monoclonal antibodies.

Declaration of interests

☒The authors declare that they have no known competing financial interests or personal relationships that could have appeared to influence the work reported in this paper.

☐The authors declare the following financial interests/personal relationships which may be considered as potential competing interests:

Highlights

- In female, but not male mice lacking PCSK9, LDLR cell surface density is greatly reduced by a specific shedding of excess LDLR. The latter differs from basal LDLR shedding, is cholesterol-dependent and may be achieved by ADAM10/17.

- PCSK9 KO male mice exhibit critically low intra-hepatic cholesterol. Excess LDLR shedding is induced in these mice by the cholesterogenic effect of 17β-estradiol (E2) mediated by the estrogen receptor alpha.

- This cholesterol-dependent LDLR shedding may explain the 15-20% lower LDL-cholesterol reduction observed in women treated with PCSK9 monoclonal antibodies.

- Low cholesterol in the liver of PCSK9 KO male mice also delay the G2/M transition of the cell cycle, a step known to be dependent on cholesterol.

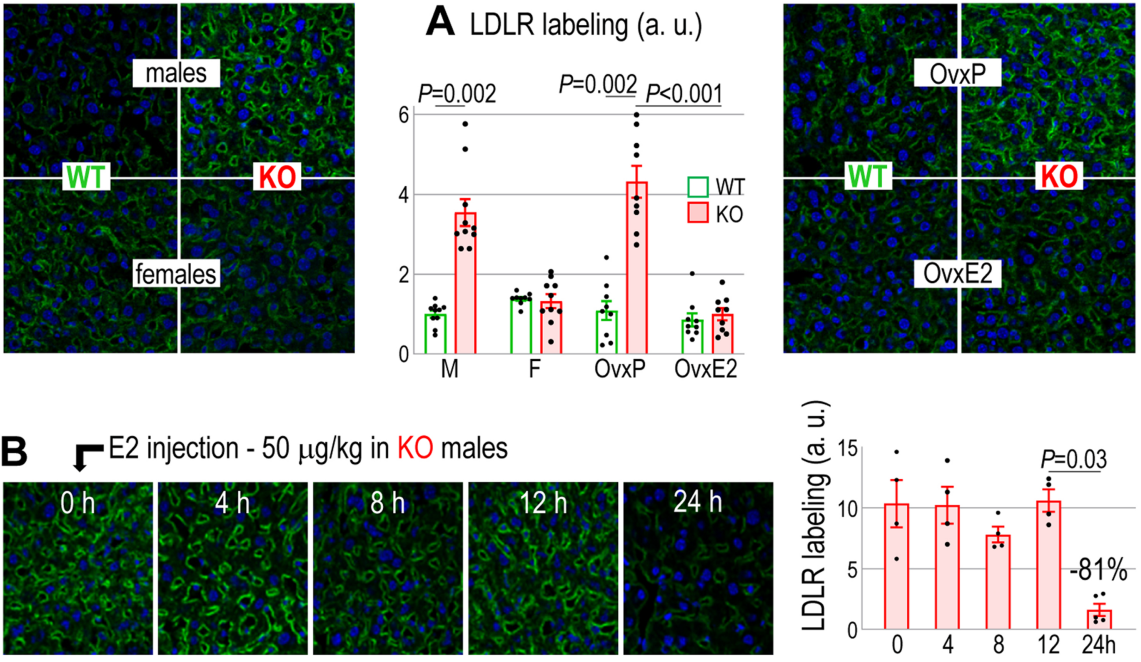
A LDLR labeling (a. u.)
males
WT
KO
females
P=0.002
P=0.002
P<0.001
WT
KO
M
F
OvxP
OvxE2
OvxP
WT
KO
OvxE2
B
E2 injection - 50 μg/kg in KO males
0 h
4 h
8 h
12 h
24 h
LDLR labeling (a. u.)
P=0.03
-81%
0
4
8
12
24h

Figure 1

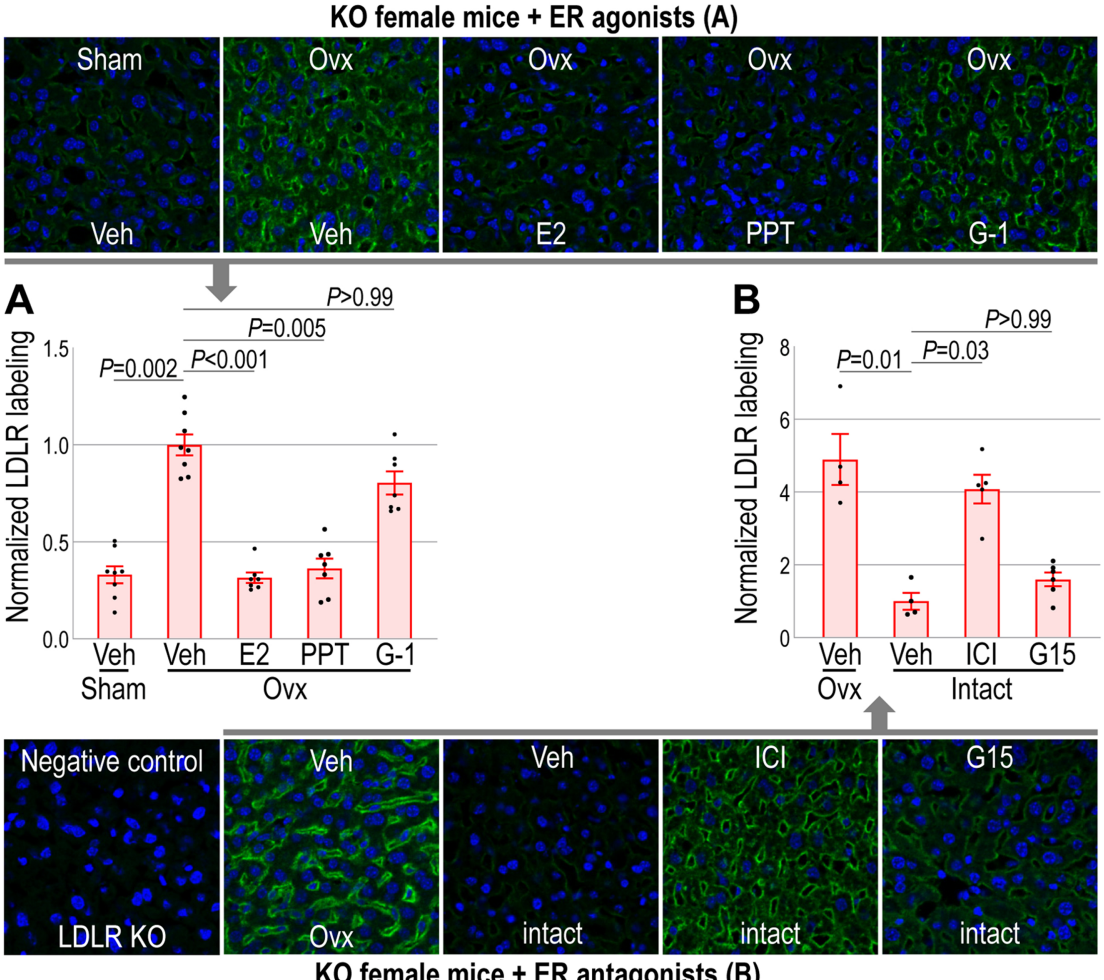
KO female mice + ER agonists (A)
Sham
Ovx
Ovx
Ovx
Ovx
Veh
Veh
E2
PPT
G-1
A
Normalized LDLR labeling
1.5
1.0
0.5
0.0
P=0.002
P<0.001
P=0.005
P>0.99
Veh
Veh
E2
PPT
G-1
Sham
Ovx
B
Normalized LDLR labeling
8
6
4
2
0
P=0.01
P=0.03
P>0.99
Veh
Veh
ICI
G15
Ovx
Intact
Negative control
Veh
Veh
ICI
G15
LDLR KO
Ovx
intact
intact
intact
KO female mice + ER antagonists (B)

Figure 2

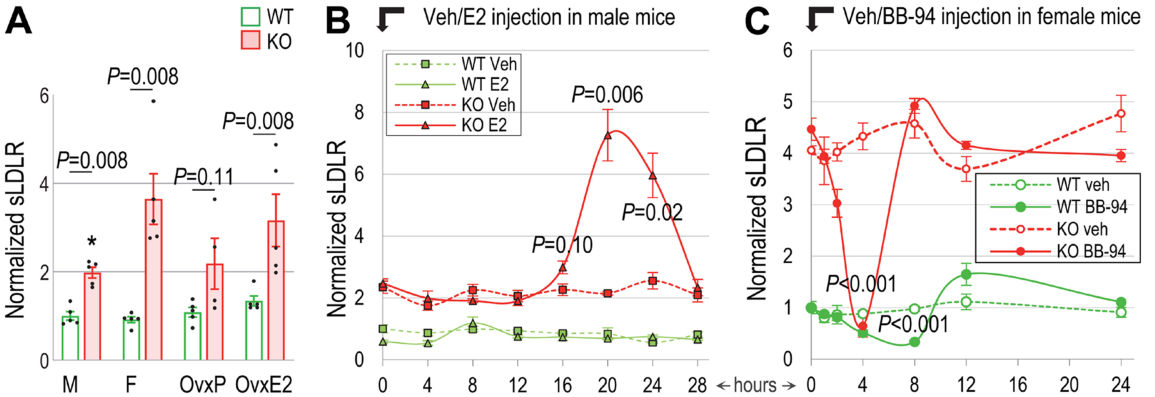
A
WT
KO
P=0.008
P=0.008
P=0.008
P=0.11
*
Normalized sLDLR
M
F
OvxP
OvxE2
B
Veh/E2 injection in male mice
WT Veh
WT E2
KO Veh
KO E2
P=0.006
P=0.02
P=0.10
Normalized sLDLR
← hours →
C
Veh/BB-94 injection in female mice
WT veh
WT BB-94
KO veh
KO BB-94
P<0.001
P<0.001
Normalized sLDLR

Figure 3

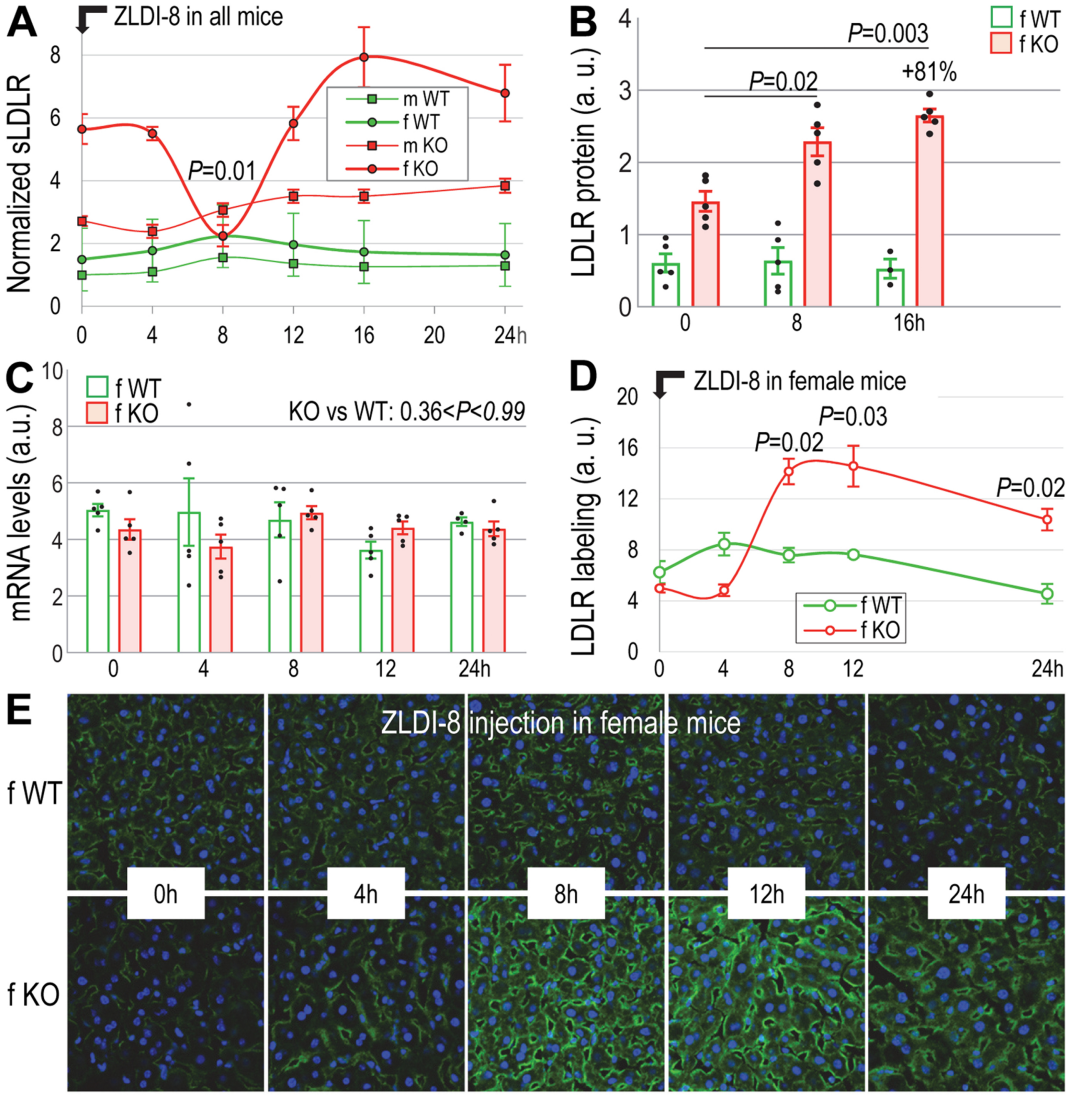
A
ZLDI-8 in all mice
Normalized sLDLR
m WT
f WT
m KO
f KO
P=0.01
0
4
8
12
16
20
24h
B
LDLR protein (a. u.)
f WT
f KO
P=0.003
P=0.02
+81%
0
8
16h
C
mRNA levels (a.u.)
f WT
f KO
KO vs WT: 0.36<P<0.99
0
4
8
12
24h
D
ZLDI-8 in female mice
LDLR labeling (a. u.)
P=0.03
P=0.02
P=0.02
f WT
f KO
0
4
8
12
24h
E
ZLDI-8 injection in female mice
f WT
f KO
0h
4h
8h
12h
24h

Figure 4

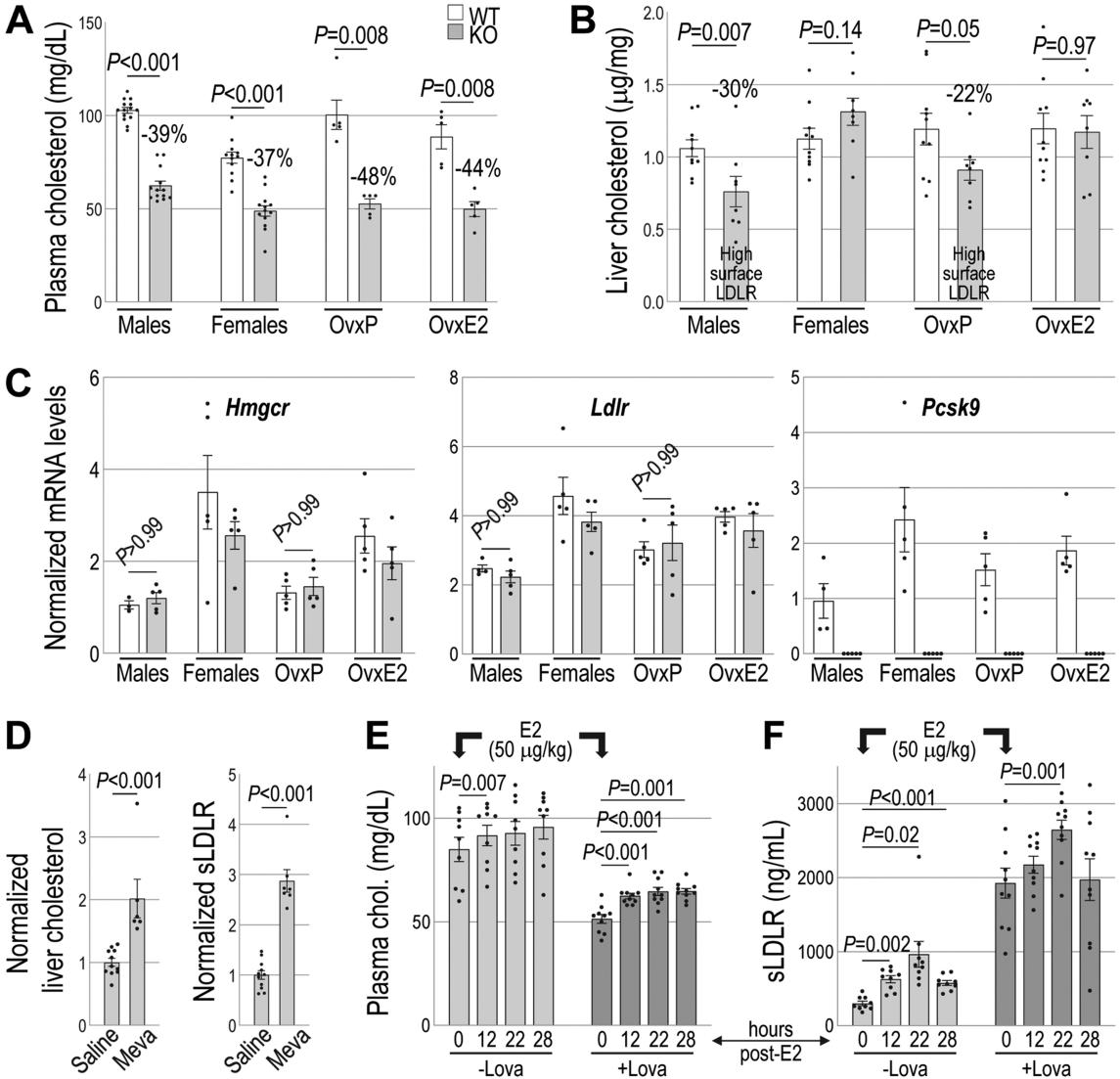
A
Plasma cholesterol (mg/dL)
WT
KO
P<0.001
-39%
P<0.001
-37%
P=0.008
-48%
P=0.008
-44%
Males
Females
OvxP
OvxE2
B
Liver cholesterol (µg/mg)
P=0.007
-30%
P=0.14
P=0.05
-22%
P=0.97
High surface LDLR
High surface LDLR
Males
Females
OvxP
OvxE2
C
Normalized mRNA levels
Hmgcr
Ldlr
Pcsk9
P>0.99
P>0.99
P>0.99
P>0.99
Males
Females
OvxP
OvxE2
D
Normalized liver cholesterol
P<0.001
Saline
Meva
Normalized sLDLR
P<0.001
Saline
Meva
E
E2 (50 µg/kg)
Plasma chol. (mg/dL)
P=0.007
P<0.001
P=0.001
P<0.001
0 12 22 28
-Lova
0 12 22 28
+Lova
hours post-E2
F
E2 (50 µg/kg)
sLDLR (ng/mL)
P<0.001
P=0.02
P=0.002
P=0.001
0 12 22 28
-Lova
0 12 22 28
+Lova

Figure 5

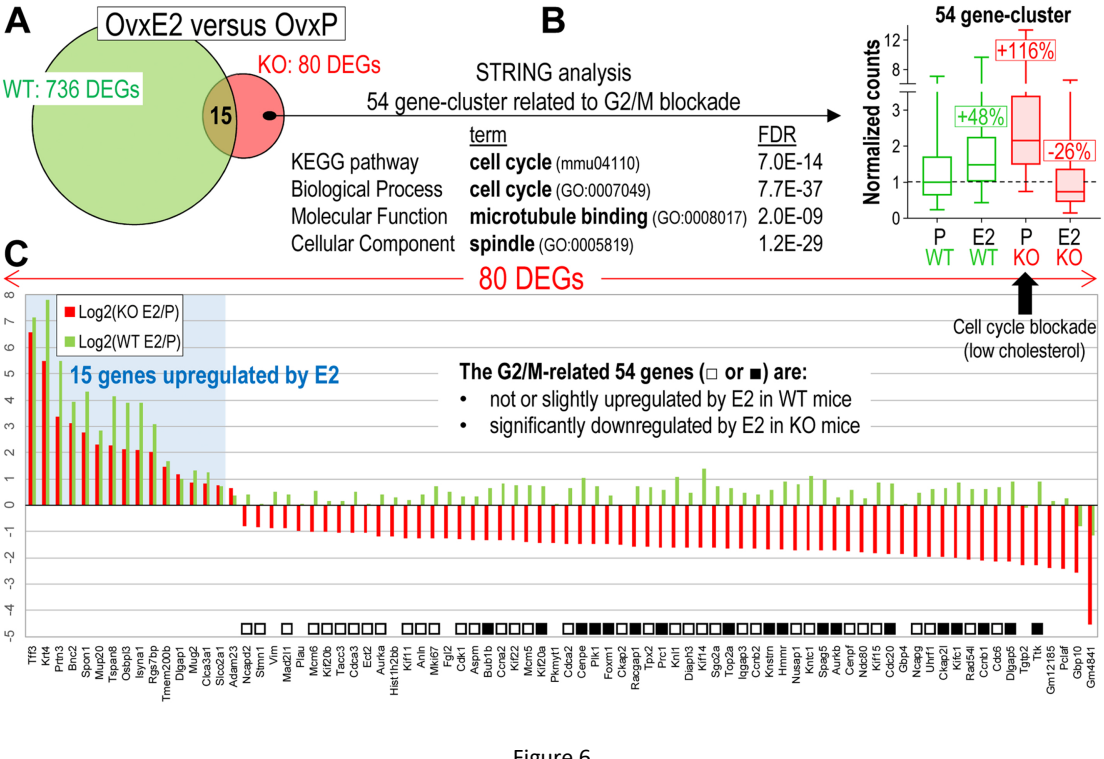
A
OvxE2 versus OvxP
WT: 736 DEGs
15
KO: 80 DEGs
B
STRING analysis
54 gene-cluster related to G2/M blockade
term
FDR
KEGG pathway cell cycle (mmu04110) 7.0E-14
Biological Process cell cycle (GO:0007049) 7.7E-37
Molecular Function microtubule binding (GO:0008017) 2.0E-09
Cellular Component spindle (GO:0005819) 1.2E-29
54 gene-cluster
Normalized counts
+116%
+48%
-26%
P WT
E2 WT
P KO
E2 KO
C
80 DEGs
Log2(KO E2/P)
Log2(WT E2/P)
15 genes upregulated by E2
The G2/M-related 54 genes (□ or ■) are:
• not or slightly upregulated by E2 in WT mice
• significantly downregulated by E2 in KO mice
Cell cycle blockade
(low cholesterol)
Tff3 Krt4 Prnp3 Bmp2 Spon1 Mug20 Tspan8 Obspl3 Isyna1 Rgs7bp Tmem200b Dlgap1 Mug2 Clca3a1 Slco2a1 Adam23 Ncapd2 Stmn1 Vim Mad2l1 Plau Mcm6 Kif20b Tacc3 Cdca3 Ect2 Aurkb Hist1h2bl Kif1 Anln Mki67 Fgl2 Cdk1 Aspm Bub1b Ccna2 Kif22 Mcm5 Kif20a Pkmyt1 Cdca2 Cenpe Plk1 Foxm1 Ckap2 Racgap1 Tpx2 Prc1 Knl1 Dlgap5 Kif14 Spc24 Top2a Iqgap3 Ccnb2 Knstrn Hmmr Nusap1 Knlc1 Spag5 Aurkb Cenpf Ndc80 Kif15 Cdc20 Gbp4 Ncapg Uhrf1 Ckap2l Kifc1 Rad54l Ccnb1 Cdc6 Dgap5 Tgm2 Ttk Gm12185 Pclaf Gbp10 Gm4841

Figure 6

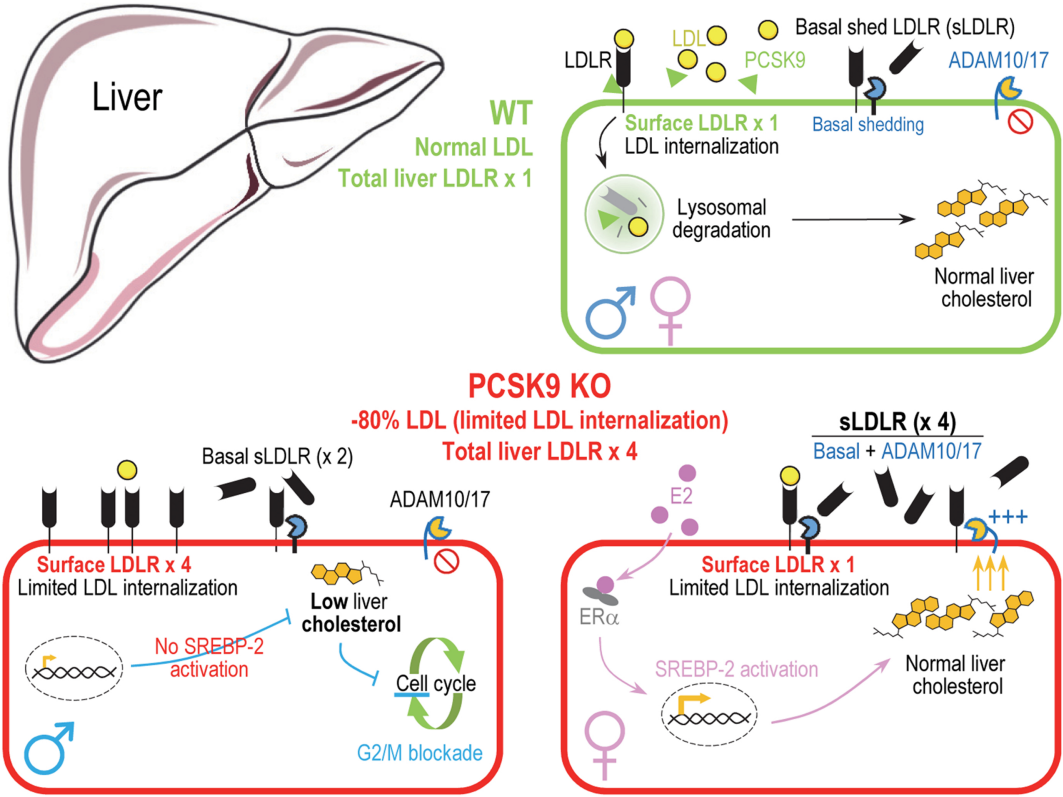
Liver
WT
Normal LDL
Total liver LDLR x 1
LDLR
LDL
PCSK9
Basal shed LDLR (sLDLR)
ADAM10/17
Surface LDLR x 1
LDL internalization
Basal shedding
Lysosomal degradation
Normal liver cholesterol
PCSK9 KO
-80% LDL (limited LDL internalization)
Total liver LDLR x 4
Basal sLDLR (x 2)
ADAM10/17
Surface LDLR x 4
Limited LDL internalization
Low liver cholesterol
No SREBP-2 activation
Cell cycle
G2/M blockade
sLDLR (x 4)
Basal + ADAM10/17
E2
+++
Surface LDLR x 1
Limited LDL internalization
ERα
SREBP-2 activation
Normal liver cholesterol

Figure 7